# Impulse Radio

Robert A. Scholtz and Moe Z. Win
Communication Sciences Institute
Department of Electrical Engineering-Systems
University of Southern California, Los Angeles, CA 90089-2565 USA

**Abstract**

Impulse radio, a form of ultra-wide band signaling, has properties that make it a viable candidate for short range communications in dense multipath environments. This paper describes the characteristics of impulse radio, gives analytical estimates of its multiple access capability, and presents propagation test results and their implications for the design of the radio receiver.

**Keywords**

Ultra-wideband Radio, Time-Hopping, Spread Spectrum, Multiple Access, Sequence Design, Multipath Channel, Propagation Measurement, Rake Reception, Diversity Combining.

The research described in this paper was supported in part by the Joint Services Electronics Program under contract F49620-94-0022, and in part by the Integrated Media Systems Center, a National Science Foundation Engineering Research Center with additional support from the Annenberg Center for Communication at the University of Southern California and the California Trade and Commerce Agency.

The authors can be reached by E-mail at scholtz@milly.usc.edu, and win@milly.usc.edu

## I. A Rationale for Impulse Radio

Typically when a baseband pulse of duration $T_{\rm m}$ seconds is transformed to the frequency domain, its energy is viewed as spanning a frequency band from d.c. up to roughly $2/T_{\rm m}$ Hz. When this pulse is applied to an appropriately designed antenna, the pulse propagates with distortion. The antennas behave as a filters, and even in free space a differentiation of the pulse occurs as the wave radiates. Impulse radio communicates with pulses of very short duration, typically on the order of a nanosecond, thereby spreading the energy of the radio signal very thinly from near d.c. to a few gigahertz.

Impulse radios, operating over the highly populated frequency range below a few gigahertz, must contend with a variety of interfering signals, and also must insure that they do not interfere with narrowband radio systems operating in dedicated bands. These requirements necessitate the use of spread-spectrum techniques. A simple means for spreading the spectrum of these ultra-wideband low-duty-cycle pulse trains is time hopping, with data modulation accomplished by additional pulse position modulation at the rate of many pulses per data bit. As a simple numerical example, suppose that an impulse radio operates over a 2 GHz bandwidth with a pulse rate of $10^6$ pulses per second at an average transmitted power level of 1 milliwatt and a data rate of $10^4$ bits per second with binary modulation. This radio then has a transmitted power spectral density of less than a microwatt per megahertz with a processing gain well over 50 dB.

Potentially there must be a real payoff in the use of impulse radio to undertake the difficult problem of coexistence with a myriad of other radio systems. For the bandwidth occupied, impulse radio operates in the lowest possible frequency range, and hence has the best chance of penetrating materials with the least attenuation. This capability, when combined with multipath resolution down to a nanosecond in differential path delay (equivalently down to a differential path length of one foot) make impulse techniques a viable technology for high quality fully mobile indoor radio systems. Lack of significant multipath fading may considerably reduce fading margins in link budgets and allow low transmission power operation. With its significant bandwidth, an impulse radio based multiple access system may accommodate many users, even in multipath environments. Monolithic implementation appears possible, implying that an impulse radio may be manufactured inexpensively.

The same qualities that make this radio attractive also provide the design challenges. Regulatory considerations over a such a wide band will limit the radiated power, ultra-fine time

resolution will increase sync acquisition times and may require additional correlators to capture adequate signal energy, full mobility will exacerbate power control needs in multiple-access networks, etc. Impulse radios have been implemented and demonstrated single-user links up to at least 150 kbps, and hence the basic principles of operation have been validated.

In the following review of impulse radio, we will survey our work on this novel technology.

## II. Multiple Access Techniques for Impulse Radio

### *A. Time-Hopping Format Using Impulses*

A typical time-hopping format employed by an impulse radio in which the $k^{\underline{\text{th}}}$ transmitter's output signal $s_{\text{tr}}^{(k)}(t^{(k)})$ is given by

$$s_{\text{tr}}^{(k)}(t^{(k)}) = \sum_{j=-\infty}^{\infty} w_{\text{tr}}(t^{(k)} - jT_{\text{f}} - c_j^{(k)}T_{\text{c}} - \delta d_{\lfloor j/N_{\text{s}} \rfloor}^{(k)}) \,, \tag{1}$$

where $t^{(k)}$ is the $k^{\underline{\text{th}}}$ transmitter's clock time, and $w_{\text{tr}}(t)$ represents the transmitted pulse waveform, referred to as a *monocycle*, that nominally begins at time zero on the transmitter's clock.

The *frame time* or *pulse repetition time* $T_{\text{f}}$ typically may be a hundred to a thousand times the monocycle width, resulting a signal with a very low duty cycle. To eliminate catastrophic collisions in multiple accessing, each user (indexed by $k$) is assigned a distinctive time-shift pattern $\{c_j^{(k)}\}$, called a *time-hopping sequence*, which provides an additional time shift to each monocycle in the pulse train. The $j^{\underline{\text{th}}}$ monocycle undergoes an additional shift of $c_j^{(k)}T_{\text{c}}$ seconds, where $T_{\text{c}}$ is the duration of addressable time delay bin. The elements $c_j^{(k)}$ of the sequence are chosen from a finite set $\{0, 1, \ldots, N_{\text{h}} - 1\}$, and hence hop-time shifts from 0 to $N_{\text{h}}T_{\text{c}}$ are possible. The addressable time-hopping duration is strictly less than the frame time since a short time interval is required to read the output of a monocycle correlator and to reset the correlator.

For performance prediction purposes, the data sequence $\{d_j^{(k)}\}_{j=-\infty}^{\infty}$ is a modeled as a wide-sense stationary random process composed of equally likely binary symbols. A pulse position data modulation is considered here in which it is assumed that the data stream is balanced so that the clock tracking loop S-curve can maintain a stable tracking point. With more complicated schemes, pulse shift balance can be achieved in each symbol time. The parameter $\delta$ is a modulation factor that can can be chosen to optimize performance. If $\delta > T_{\text{m}}$, then the transmitted signals representing 0 and 1 are orthogonal.

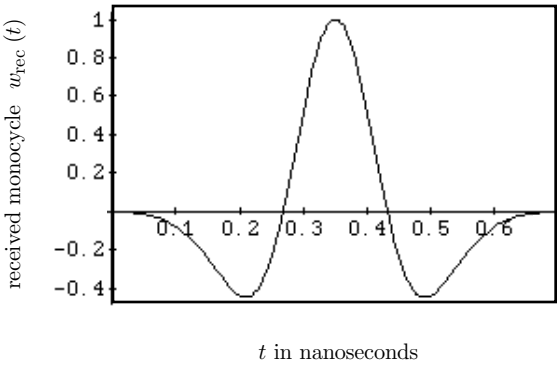


Fig. 1. A typical received monocycle $w_{\rm rec}(t)$ at the output of the antenna subsystem as a function of time in nanoseconds.

### *B. The Multiple Access Channel*

When $N_{\rm u}$ users are active in the multiple-access system, the composite received signal $r(t)$ at the output of this receiver's antenna is modeled as

$$r(t) = \sum_{k=1}^{N_{\rm u}} A_k s_{\rm rec}^{(k)}(t - \tau_k) + n(t)\,, \tag{2}$$

in which $A_k$ models the attenuation over the propagation path of the signal, $s_{\rm rec}^{(k)}(t-\tau_k)$, received from the $k^{\underline{\rm th}}$ transmitter. The random variable $\tau_k$ represents the time asynchronism between the clock of transmitter $k$ and the receiver, and $n(t)$ represents other non-monocycle interference (e.g., receiver noise) present at the correlator input.

The number of transmitters $N_{\rm u}$ on the air and the signal amplitudes $A_k$ are assumed to be constant during the data symbol interval. The propagation of the signals from each transmitter to the receiver is assumed to be ideal, each signal undergoing only a constant attenuation and delay. The antenna/propagation system modifies the shape of the transmitted monocycle $w_{\rm tr}(t)$ to $w_{\rm rec}(t)$ at its output. An idealized received monocycle shape $w_{\rm rec}(t)$ for a free-space channel model is shown in Fig. 1. This channel model ignores multipath, dispersive effects, etc.

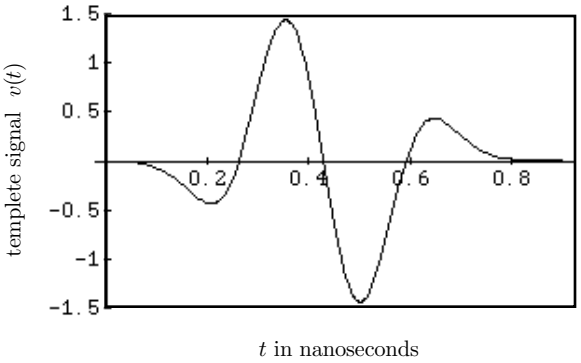


Fig. 2. The template signal $v(t)$ with the modulation parameter $\delta$ chosen to be 0.156 ns. Since the template is a difference of two pulses shifted by $\delta$, the non-zero extent of the template signal is approximately $\delta$ plus the monocycle width, i.e., about 0.86 ns.

### *C. Impulse Radio Receiver Signal Processing*

The optimum receiver for a single bit of a binary modulated impulse radio signal in additive white Gaussian noise is a correlation receiver [1],[2],[3], which can be reduced to

$$\text{"decide } d_0^{(1)} = 0\text{"} \iff \underbrace{\sum_{j=0}^{N_\mathrm{s}-1} \overbrace{\int_{\tau_1+jT_\mathrm{f}}^{\tau_1+(j+1)T_\mathrm{f}} r(t)v(t-\tau_1-jT_\mathrm{f}-c_j^{(1)}T_\mathrm{c})dt}^{\text{pulse correlator output } \triangleq\ \alpha_j}}_{\text{test statistic } \triangleq\ \alpha} \ > \ 0\,, \tag{3}$$

where the *correlation template signal* is $v(t) \triangleq w_{\mathrm{rec}}(t) - w_{\mathrm{rec}}(t-\delta)$.

The optimal detection in a multi-user environment, with knowledge of all time-hopping sequences, leads to complex receiver designs [4], [5]. However, if the number of users is large and no such multi-user detector is feasible, then it is reasonable to approximate the combined effect of the other users' dehopped interfering signals as a Gaussian random process [1], [6]. Hence the single-link reception algorithm (3) is used here as a theoretically tractable receiver model, amenable as well to practical implementations.

The test statistic $\alpha$ in (3) consists of summing the $N_\mathrm{s}$ correlations $\alpha_j$ of the correlator's template signal $v(t)$ at various time shifts with the received signal $r(t)$. The signal processing corresponding to this decision rule in (3) is shown in Fig. 3. A graph of the template signal is shown in Fig. 2 using the typical received waveform given in Fig. 1.

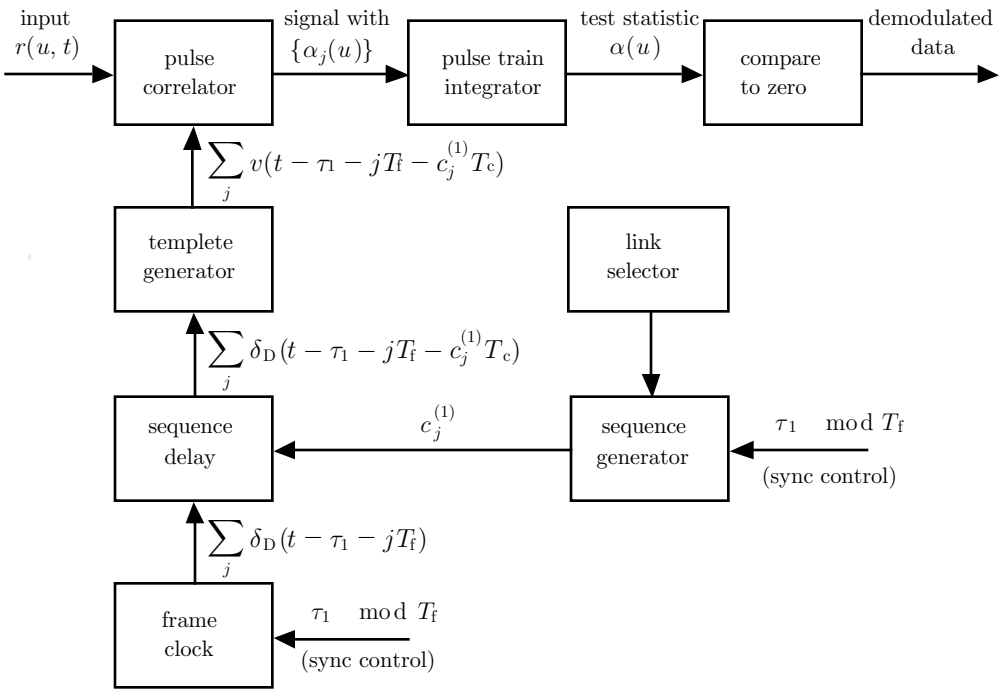


Fig. 3. Receiver block diagram for the reception of the first user's signal. Clock pulses are denoted by Dirac delta functions $\delta_{\rm D}(\cdot)$.

### *D. Multiple Access Performance*

Using the approach of [7], the average output signal-to-noise ratio of the impulse radio is calculated in [1] for randomly selected time-hopping sequences as a function of the number of active users $N_{\rm u}$ as

$$SNR_{\rm out}(N_{\rm u}) = \frac{(N_{\rm s}A_1 m_{\rm p})^2}{\sigma_{\rm rec}^2 + N_{\rm s}\sigma_{\rm a}^2 \sum_{k=2}^{N_{\rm u}} A_k^2}\,. \tag{4}$$

Here $\sigma_{\rm rec}^2$ is the variance of the receiver noise component at the pulse train integrator output. The monocycle waveform-dependent parameters $m_{\rm p}$ and $\sigma_{\rm a}^2$ in (4) are given by

$$\begin{aligned} m_{\rm p} &= \int_{-\infty}^{\infty} w_{\rm rec}(x-\delta)v(x)dx, \qquad \text{and} \\ \sigma_{\rm a}^2 &= T_{\rm f}^{-1}\int_{-\infty}^{\infty}\left[\int_{-\infty}^{\infty} w_{\rm rec}(x-s)v(x)dx\right]^2 ds\,, \end{aligned}$$

respectively.

The $SNR_{\rm out}(N_{\rm u})$ of the impulse radio can be rewritten as

$$SNR_{\rm out}(N_{\rm u}) = \left\{ SNR_{\rm out}^{-1}(1) + M\sum_{k=2}^{N_{\rm u}}\left(\frac{A_k}{A_1}\right)^2 \right\}^{-1}, \tag{5}$$

where the parameter $M$ is given by

$$M^{-1} \triangleq \frac{N_{\rm s} m_{\rm p}^2}{\sigma_{\rm a}^2}\,. \tag{6}$$

Let's suppose that a specified signal-to-noise ratio $SNR_{\rm spec}$ must be maintained for the link to satisfy a performance specification. If this specification is to be met when $N_{\rm u}-1$ other users are active, then it follows that $SNR_{\rm out}(1)$ in (5) represents the required equivalent single link signal-to-noise ratio (ignoring multiple access noise) such that $SNR_{\rm out}(N_{\rm u}) = SNR_{\rm spec}$. Therefore the ratio of $SNR_{\rm out}(1)$ to $SNR_{\rm out}(N_{\rm u}) = SNR_{\rm spec}$ represents the fractional increase in every transmitter's power that is required to maintain its signal-to-noise ratio at a level $SNR_{\rm spec}$ in its receiver in the presence of multiple-access interference caused by $N_{\rm u}-1$ other users. We define the fractional increase in required power (in units of dB) as $\Delta P \triangleq 10\log_{10}\{SNR_{\rm out}(1)/SNR_{\rm spec}\}$.

Under the assumption of perfect power control, the number of users that the multiple access impulse radio system can support on an aggregate additive white Gaussian noise channel for a given data rate is shown in [8] to be

$$N_{\rm u}(\Delta P) = \left\lfloor M^{-1} SNR_{\rm spec}^{-1}\left\{1 - 10^{-(\Delta P/10)}\right\}\right\rfloor + 1\,, \tag{7}$$

which is a monotonically increasing function of $\Delta P$. Therefore

$$\begin{aligned} N_{\rm u}(\Delta P) &\leq \lim_{\Delta P\to\infty} N_{\rm u}(\Delta P) \\ &= \left\lfloor M^{-1} SNR_{\rm spec}^{-1}\right\rfloor + 1 \triangleq N_{\max}\,. \end{aligned} \tag{8}$$

Hence the number of users at a specified bit-error rate (BER) based on $SNR_{\rm spec}$ cannot be larger than $N_{\max}$, no matter how large the power of each user's signal is. In other words, when the number of active users is more than $N_{\max}$, then the receiver can not maintain the specified level of performance regardless of the additional available power. Similar results for direct sequence code division multiple-access systems can be found in [7].

### *E. A Performance Evaluation Example*

The performance of the impulse radio receiver in a multiple-access environment is evaluated using a specific example. The duration of a single symbol used in this example is $T_{\rm s} = N_{\rm s} T_{\rm f}$. For a fixed frame (pulse repetition) time $T_{\rm f}$, the *symbol rate* $R_{\rm s}$ determines the number $N_{\rm s}$ of monocycles that are modulated by a given binary symbol via the equation $R_{\rm s} = \frac{1}{T_{\rm s}} = \frac{1}{N_{\rm s} T_{\rm f}}$ sec$^{-1}$.

The modulation parameter $\delta$ in (1), which affects the shape of the template signal $v(t)$, affects performance only through $m_{\rm p}$ and $\sigma_{\rm a}^2$ implicitly, and can be adjusted to maximize $SNR_{\rm out}(N_{\rm u})$ under various conditions. When the receiver noise dominates the multiple-access noise, e.g., when there is only one user or when there is a strong external interferer, then it can be shown that the optimum choice of modulation parameter is the one that maximizes $|m_{\rm p}|$. On the other hand, when the receiver noise is negligible and $SNR_{\rm out}(1)$ is nearly infinite, then the optimum choice of $\delta$, suggested by (4), is the one that maximizes $|m_{\rm p}|/\sigma_{\rm a}$. For the monocycle waveform of Fig. 1 which we will use in this example, these considerations imply that $\delta$ should be chosen as either 0.144 ns or 0.156 ns, and little is lost in choosing either of these values. Choosing $\delta = 0.156$ ns and $T_{\rm f} = 100$ ns, then $m_{\rm p} = -0.1746$, $\sigma_{\rm a}^2 = 0.006045$, and the unitless constant that is required for calculating $M^{-1}$ in (6) is $m_{\rm p}^2/\sigma_{\rm a}^2 \approx 504$. With a data rate $R_{\rm s} = 19.2$ kbps, the quantity $M^{-1}$ is calculated to be $2.63 \times 10^5$.

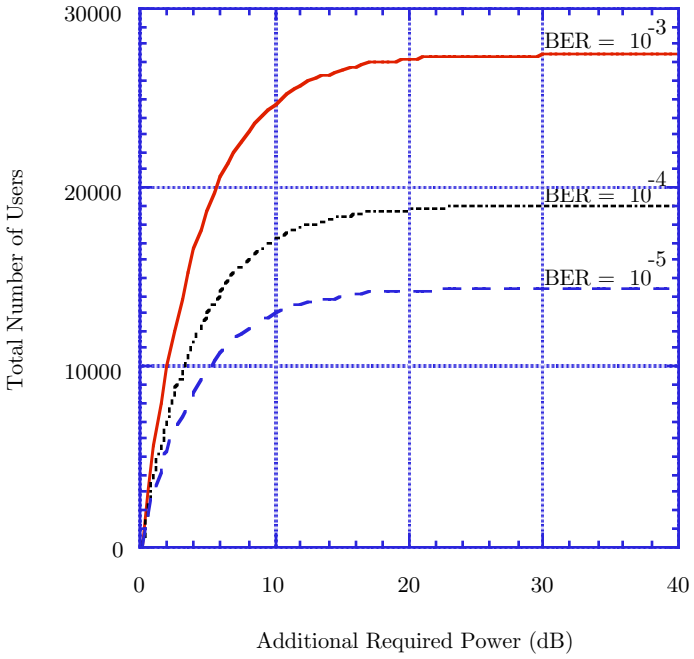


Fig. 4. Total number of users versus additional required power (dB) for the impulse radio example. Ideal power control is assumed at the receiver. Three different bit error rate performance levels with the data rate set at 19.2 Kbps are considered.

The number of users versus additional required power $\Delta P$ for multiple access operation with ideal power control is plotted for typical BERs in Fig. 4 for this example. To maintain BER of

$10^{-3}$, $10^{-4}$, and $10^{-5}$ in a communications system with no error control coding, $SNR_{\text{spec}}$ must be 12.8 dB, 14.4 dB, and 15.6 dB respectively. Note that the number of users increases rapidly as $\Delta P$ increases from 0 to 10 dB. However, this improvement becomes gradual as $\Delta P$ increases from 10 to 20 dB. Beyond this point, only negligible improvement can be made as $\Delta P$ increases and $N_{\text{u}}$ approaches $N_{\max}$. In practice, impulse radios are expected to operate in regions where the increase in the number of users as a function of $\Delta P$ is rapid. The values of $N_{\max}$ is calculated to be 27488, 19017, and 14426 for BERs of $10^{-3}$, $10^{-4}$, and $10^{-5}$ respectively, and these are the asymptotic values on the curves in Fig. 4. It is worth noting that if a direct sequence CDMA system with roughly the same bandwidth were analyzed, one would find comparable numbers of users in the same communication environment.

### *F. Comments on Sequence Design*

The above performance evaluation is based on average results for randomly selected time-hopping sequence designs. In reality some sort of pseudonoise generator must provide transmitter and receiver with, previously agreed upon, time-hopping sequences for each communication link. Techniques for providing sets of sequences with good Hamming correlation are well known [9] and may be adapted to the time-hopping application to provide quasi-orthogonal signaling schemes.

The ability of the receiver to reject narrowband interference and the ability of the transmitter to avoid interfering with other radio systems depends on the power spectral density of the time-hopped monocycle pulse trains. For a given periodic pseudorandom time-hopping sequence $\{c_j^{(k)}\}$, the power spectral density $S_{\text{tr}}(f)$ of a time-hopped signal $s_{\text{tr}}^{(k)}(t^{(k)})$ in a absence of data modulation of can be computed as

$$S_{\text{tr}}(f) = \frac{|W(f)|^2}{T_{\text{p}}^2} \underbrace{\left| \sum_{n=0}^{N_{\text{p}}-1} \exp\{-j2\pi f(nT_{\text{f}} + c_n T_c)\} \right|^2}_{\triangleq\, C(f)} \sum_{k=-\infty}^{\infty} \delta_D(f - k/T_{\text{p}})\,. \tag{9}$$

Notice that the delta functions which compose the line spectral density are now separated by the reciprocal of one period ($\frac{1}{T_{\text{p}}}$) of the pseudorandomly time-hopped signal. This narrower spectral line spacing provides an opportunity to spread the power more evenly across the band and to minimize the amount of power that any single spectral line can represent. The addition of non-trivial data modulation on the signal will further smooth this line spectral density as a function of frequency.

The envelope of the lines in the spectral density has two frequency-dependent factors, namely $|W(f)|^2$ and $C(f)$, the latter being time-hopping sequence dependent. Note that when $T_{\rm f}$ is a integer multiple of $T_{\rm c}$, $C(f)$ is periodic in $f$ with period $1/T_{\rm c}$, so attempts to influence one portion of the frequency spectrum by sequence design will have an affect on another portion of the spectrum. There may be an opportunity to make $C(f)$ better than approximately flat as a function of frequency, e.g., make $C(f) \approx 1/|W(f)|^2$ over a specified interval.

There may be some lines in the power spectral density which cannot be reduced by clever design of time-hopping sequence. For example, suppose that $T_{\rm f}/T_{\rm c} = m'/n'$, where $m'$ and $n'$ are relatively prime integers. Then $C(f) = N_{\rm p}^2$ for all frequencies $f$ that are integer multiples of $n'/T_{\rm c}$, and lines exist in $S_{\rm tr}(f)$ at these frequencies. The heights of these spectral lines are independent of the time-hopping sequence and can only be influenced by the energy spectrum $|W(f)|^2$ of the monocycle waveform.

## III. Design for Indoor Multipath

Analysis for the aggregate additive white Gaussian noise channel is a reasonable way to obtain an initial understanding of how a communication link works, but does not accurately predict performance in a complicated propagation environment. We will now describe ultra-wideband propagation measurements of indoor communication channels, and their use in impulse radio design.

### *A. Propagation Measurement Technique*

The measurement technique employed here is to probe the channel periodically with a sub-nanosecond pulse and to record the response of the channel with a digital sampling oscilloscope (DSO). Path resolution is possible down to about 1 ns of differential delay, corresponding to about one foot differential path length, without special processing. The repetition rate of the pulses is $2 \times 10^6$ pulses per second, implying that multipath spreads up to 0.5 microsecond can be observed unambiguously.

A diagram of the measurement apparatus is shown in Fig. 5. One of the three ultra-wideband antennas is set in close proximity to the transmit antenna to supply a trigger signal to the DSO over a long fixed length coaxial cable. Therefore, all recorded multipath profiles have the same absolute delay reference, and time delay measurements of the signals arriving to the receiving antenna via different propagation paths can be made. During each of the multipath profile

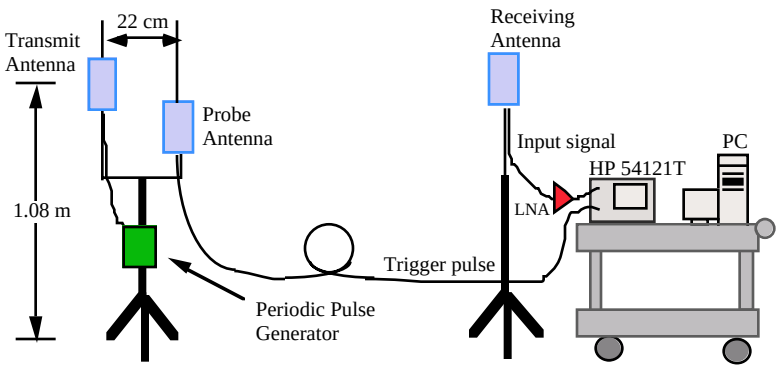


Fig. 5. A block diagram of the measurement apparatus.

measurements, both the transmitter and receiver are kept stationary.

### *B. Measurement Results*

Propagation measurements were made on one floor of a modern laboratory/office building having the floor plan shown in Fig. 6. Each of the rooms is labeled alphanumerically. Walls around offices are framed with metal studs and covered with plaster board. The wall around the laboratory is made from acoustically silenced heavy cement block. There are steel core support pillars throughout the building, notably along the outside wall and two within the laboratory itself. The shield room's walls and door are metallic. The transmitter is kept stationary in the central location of the building near a computer server in a laboratory denoted by F. The transmit antenna is located 165 cm from the floor and 105 cm from the ceiling.

Figure 7 shows the transmitted pulses measured by the receiving antenna, located 1 m away from the transmit antenna at the same height. Measurements were made while the vertically polarized receiving antenna is rotated about its vertical axis in 45° steps (see Fig. 7). The antenna, which is flat and roughly the size of a playing card, displays nearly circularly symmetric patterns about its vertical axis. The building layout diagram of Fig. 6 indicates that the closest object to the measurement apparatus is the south wall of laboratory F, which is at least 1 meter away. The signal arriving at the receiving antenna, except for the line-of-sight (LOS) signal, must travel a minimum distance of 3 meters. The initial multipaths come from the floor and ceiling, 5.2 ns and 4.1 ns after the LOS signal respectively, and hence the first 10 ns of the recorded waveforms in Fig. 7 represent clean pulse arriving via the direct LOS path and not corrupted by

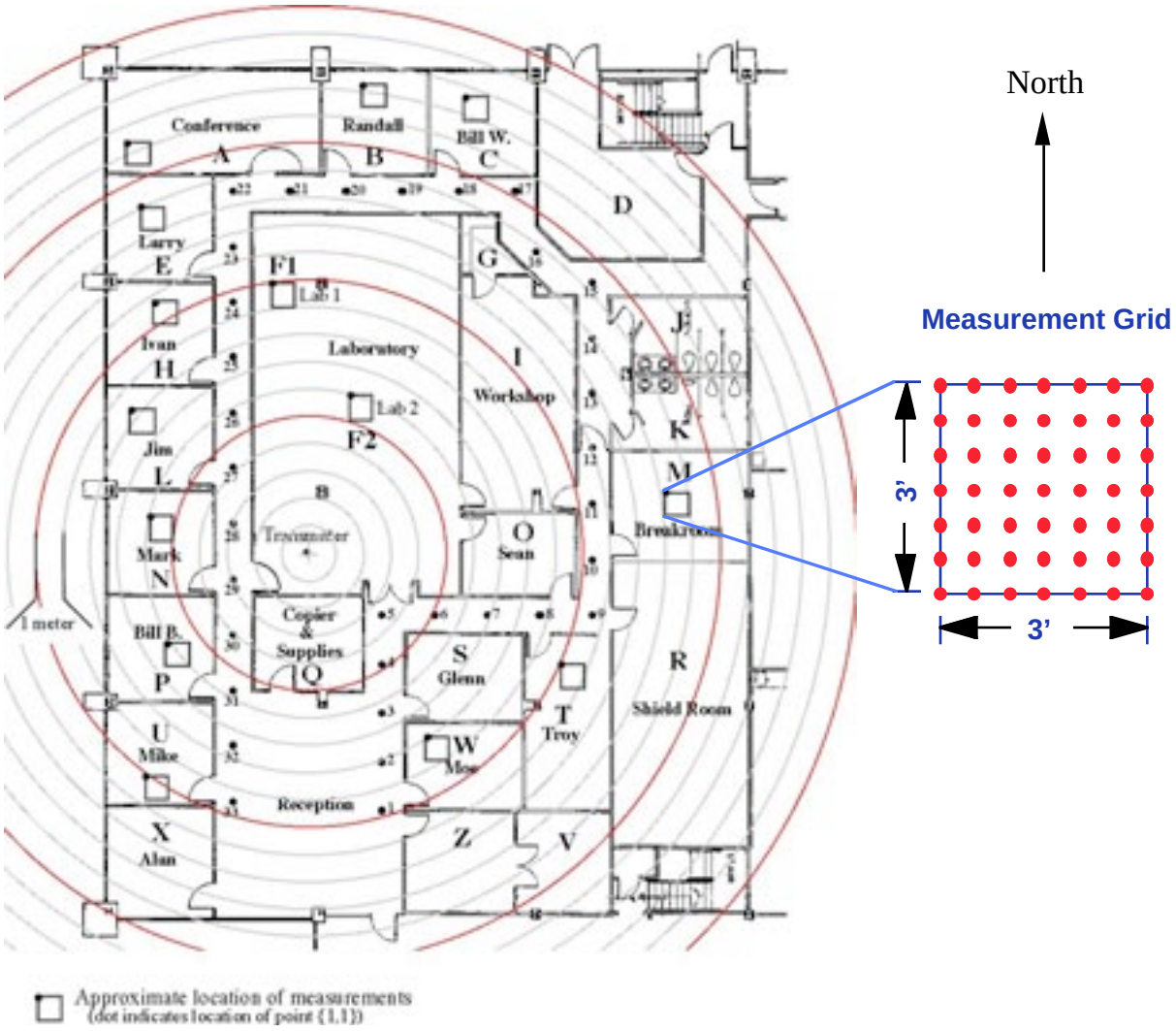


Fig. 6. The layout diagram of a typical modern office building where the propagation measurement experiment was performed. The concentric circles are centered on the transmit antenna and are spaced at 1 meter intervals.

multipath components.

Multipath profiles are measured at various locations (see Fig. 6) in 14 rooms and hallways throughout the building. In each room, 300 ns long response measurements are made at 49 different locations over a 3 feet by 3 feet square grid with 6 inch spacing between measurement points. One side of the grid is always parallel to north wall of the room. The receiving antenna is located 120 cm from the floor and 150 cm from the ceiling.

Profiles measured over one microsecond in offices U, W, and M are shown in Fig. 8. The

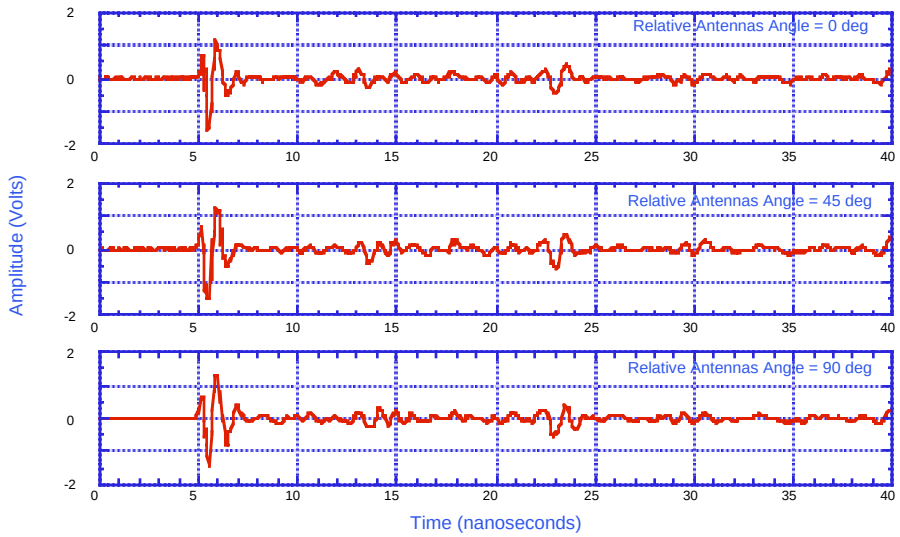


Fig. 7. Transmitted pulses measured by the receiving antenna located 1 m away from the transmit antenna with the same height. Measurements were made while the vertically polarized receiving antenna is rotated about its axis, where 0° refers to the case in which the transmit and the receiving antennas are facing at each other.

approximate distances between the transmitter and the locations of these measurements are 10, 8.5, and 13.5 meters respectively. Figure 8 also shows that the response to the first probing pulse has decayed almost completely in roughly 200 ns, and has disappeared before the response to the next pulse arrives at the antenna. The multipath profiles recorded in the offices W and M have a substantially lower noise floor than those recorded in office U. This is explained, with the help of Fig. 6, by observing that Office U is situated at the edge of the building with a large glass window and is subject to more external interference, while Offices W and M are situated roughly in the middle of the building. Furthermore, offices W and M are near to room R which is shielded from electromagnetic radiation. Interference from radio stations, television stations, cellular and paging towers, and other external electromagnetic interference (EMI) sources are attenuated by the shielded walls and multiple layers of other regular walls. In general, an increased noise floor is observed for all the measurements made in offices located at edges of the building with large glass windows.

Figure 9 shows the averaged multipath profiles measured in office P and H at three different aligned positions one foot apart in the measurement grid. The positions of the receiving antenna

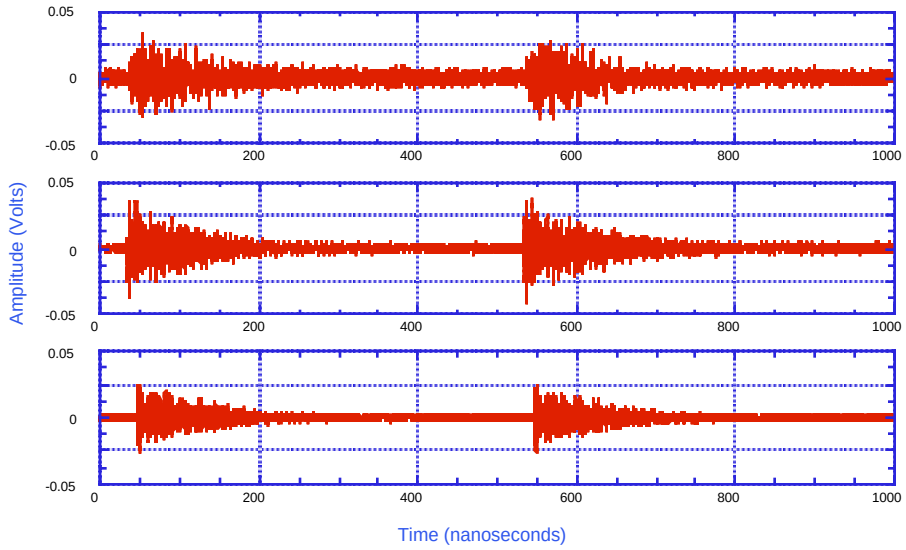


Fig. 8. Average multipath measurements of 32 sequentially measured multipath profiles where the receiver is located at the same exact locations in offices U (upper trace), W (middle trace), and M (lower trace) where the measurement grids are 10, 8.5, and 13.5 meters away from the transmitter respectively.

in rooms P and H are located 6 and 10 meters away from the transmitter respectively, representing typical UWB signal transmission for the "high SNR," and "low SNR" environments. Since there are walls and reflectors along the line of sight, the direct path response cannot be isolated from multipath. Notice that the leading edge of the direct path response suggests that the location of the receiver for the lower trace is closer to the transmitter than that of the upper trace.

To understand the effect of office doors, two multipath profiles were recorded at the same location in office B, one with the office door open and the other with the office door closed. No noticeable difference between these two measurements was observed. The effect of the large computer monitor was also considered. When the receiving antenna was placed near a large computer monitor in office C, a slight increase in noise floor was observed when the computer monitor was turned on.

### *C. Robustness in Multipath*

Robustness of the impulse radio signal to multipath can be assessed by measuring the received energy in various locations of the building relative to the received energy at a reference point.

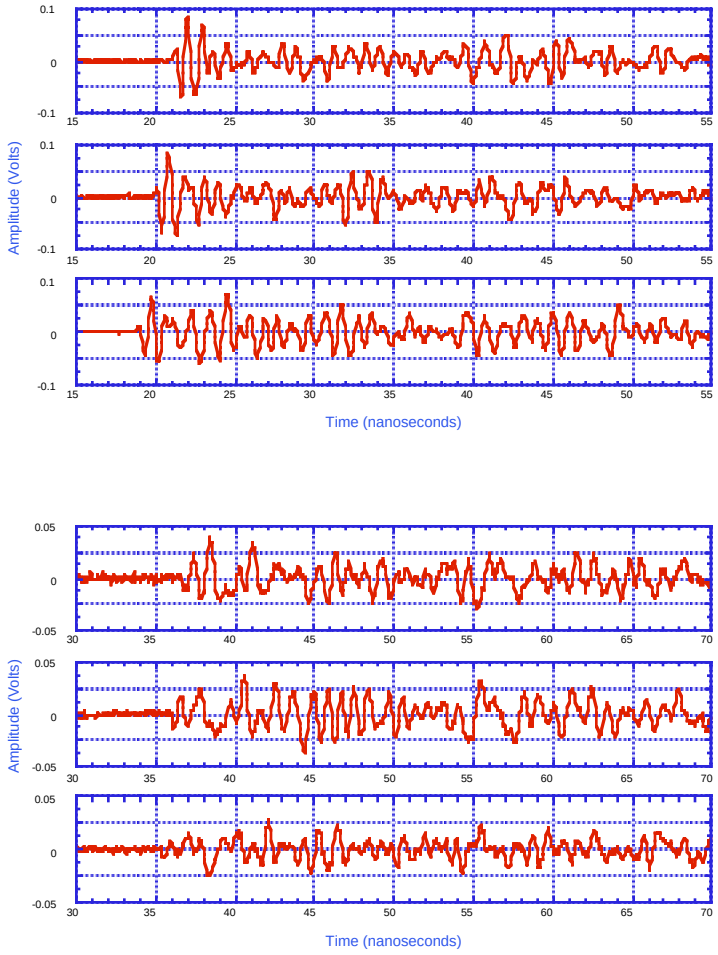


Fig. 9. Averaged multipath profiles of 40 ns window measured in rooms P (top three traces) and H (bottom three traces) along the horizontal cross section of the grid at three different aligned positions of one foot apart. The positions of the receiving antenna in rooms P and H are located 6 and 10 meters away from the transmitter respectively, representing typical UWB signal transmission for the "high SNR," and "low SNR" environments.

Mathematically, the *signal quality* at measurement grid location $(i, j)$ can be defined as

$$Q_{i,j} = 10 \log_{10} E_{i,j} - 10 \log_{10} E_{\text{ref}} \qquad [\text{d}B]\,. \tag{10}$$

The received energy $E_{i,j}$ at a location $(i, j)$ is given by

$$E_{i,j} = \int_0^T |r_{i,j}(t)|^2 dt, \tag{11}$$

where $r_{i,j}(t)$ is the measured multipath profile at location $(i, j)$ in the grid and $T$ is the observation time. The reference energy $E_{\text{ref}}$ is chosen to be the energy in the LOS path measured by the

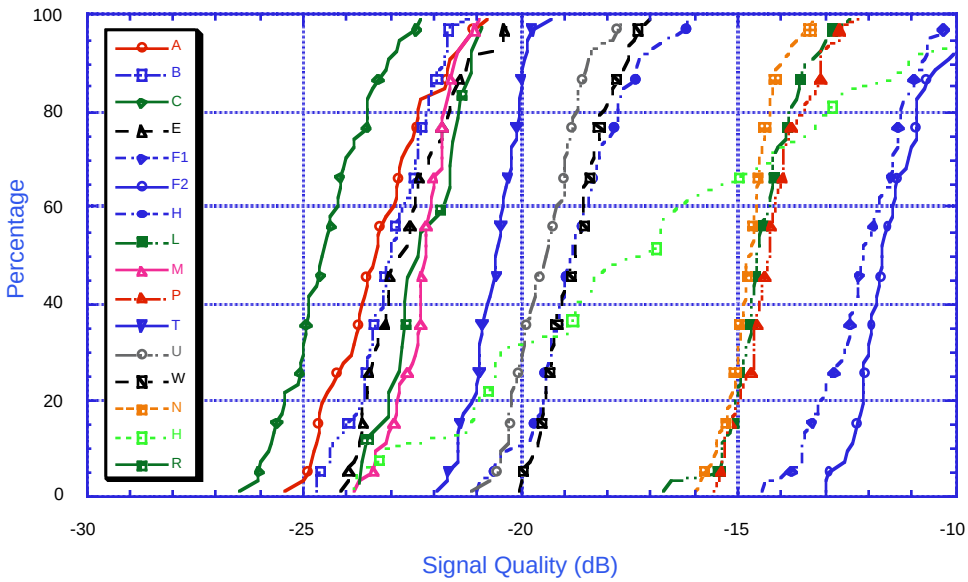


Fig. 10. The cumulative distribution function of the signal quality based on 49 spatial sample points (except 21 spatial points for room R, and 34 spatial points for hall ways) in each room. A total of 741 measurements are used in this plot.

receiver located 1 meter away from the transmitter.

The signal quality $Q_{i,j}$ is calculated for the measurements made at 741 different locations (14 different rooms with 49 locations/room, 21 locations in the shield room, and 34 locations in the hall ways).

Table I shows the estimates of the mean and the variance of the signal quality in each room based on the samples taken in that area. The cumulative distribution function of the signal quality for measurements made in these locations are shown in Fig. 10. This data indicates that the signal energy per received multipath waveform varies by at most 5 dB as the receiving position varies over the measurement grid within a room. This is considerably less than the fading margin in narrowband systems, and indicates the potential of impulse radio and ultra-wideband radios in general for robust indoor operation at low transmitted power levels.

### *D. Infinite Rake Receiver*

The ultimate goal of a Rake receiver is to construct correlators or filters that are matched to the set of symbol waveforms that it must process. If the propagation measurement process

TABLE I

Signal Quality Statistics

| Office | distance (meters) | Minimum (dB) | Maximum (dB) | $\hat{\mu}$ (dB) | Median (dB) | $\hat{\sigma}$ (dB) | # of Samples |
|---|---|---|---|---|---|---|---|
| F2 | 5.5 | -12.9970 | -9.64586 | -11.5241 | -11.6813 | 0.8161 | 49 |
| N | 5.5 | -16.0060 | -13.2949 | -14.7260 | -14.7690 | 0.5892 | 49 |
| P | 6.0 | -15.5253 | -12.2185 | -14.2373 | -14.2820 | 0.8091 | 49 |
| L | 8.0 | -16.6966 | -12.4310 | -14.4500 | -14.5538 | 0.8342 | 49 |
| W | 8.5 | -20.0157 | -17.0351 | -18.7358 | -18.7425 | 0.7622 | 49 |
| F1 | 9.5 | -14.4064 | -9.79770 | -12.0986 | -12.1407 | 1.0563 | 49 |
| H | 10.0 | -21.0415 | -16.1628 | -18.7141 | -18.8142 | 1.1240 | 49 |
| U | 10.0 | -21.1719 | -17.6232 | -19.4275 | -19.4092 | 0.8024 | 49 |
| T | 10.5 | -21.9113 | -19.2986 | -20.6100 | -20.5419 | 0.5960 | 49 |
| R | 10.5 | -23.7221 | -20.8867 | -22.2675 | -22.3851 | 0.8686 | 21 |
| M | 13.5 | -23.8258 | -20.9277 | -22.2568 | -22.2064 | 0.6439 | 49 |
| E | 13.5 | -24.1454 | -20.2000 | -22.5973 | -22.7824 | 1.0332 | 49 |
| A | 16.0 | -25.4171 | -20.7822 | -23.2826 | -23.3541 | 1.1512 | 49 |
| B | 17.0 | -24.7191 | -21.2006 | -22.9837 | -22.9987 | 0.8860 | 49 |
| C | 17.5 | -26.4448 | -22.3120 | -24.4842 | -24.5777 | 1.0028 | 49 |
| Hallways | | -23.8342 | -6.72469 | -16.9317 | -17.3286 | 4.5289 | 34 |

is carried out by sounding the channel with the monocycle $w_{\rm tr}(t)$ from which an impulse radio constructs its time-hopping signal, then the measurements can be used directly to estimate the performance of the receiver and to carry out various aspects of the receiver design.[1] We use the term *infinite Rake (IRake)* to describe a receiver with unlimited resources (correlators) and infinitely fast adaptability, so that it can, in principle, construct matched filters or correlators arbitrarily well.

The performance of any ideal synchronous receiver operating over a single-link additive white Gaussian noise channel depends on the autocorrelation matrix of the signal set. Assuming that

[1]Note that the measurements reported in Section III were made with pulse generator having wider pulse width than the pulse waveform model used in Fig. 1 and Section II.

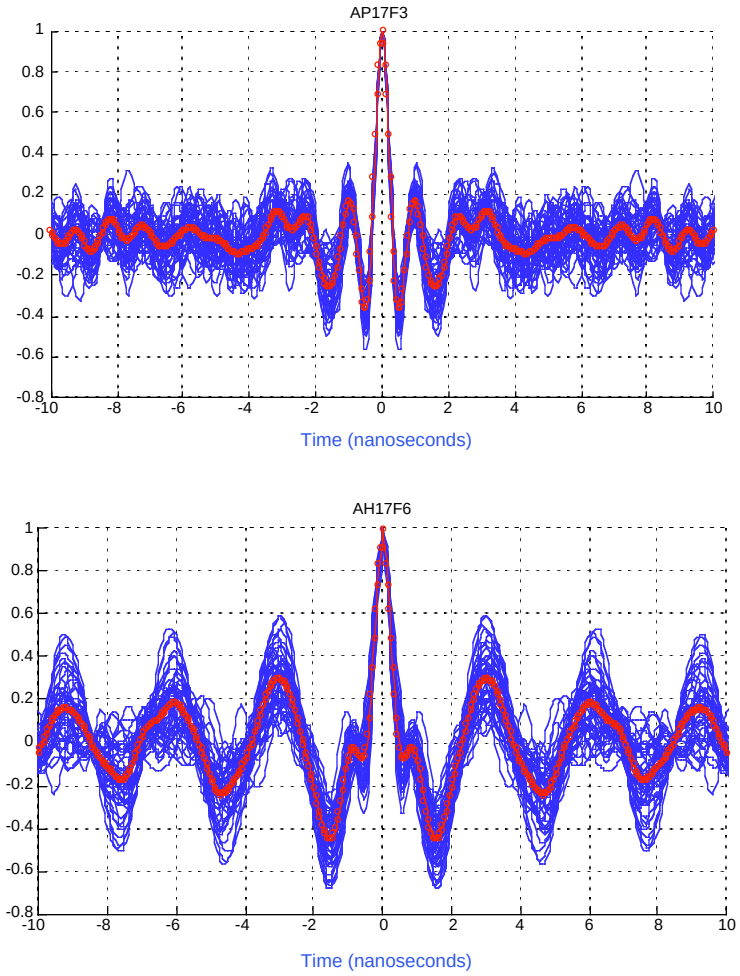


Fig. 11. Joint normalized plot of 49 different $R_{\mathrm{IRake}}(\zeta)$ functions obtained in rooms P (upper plot) and H (lower plot).

the multipath spread plus the maximum time-hop delay is less than the pulse repetition time, no intersymbol or interpulse interference is present and the performance of a perfectly synchronized impulse radio in such multipath can be predicted from the autocorrelation function $R_{\mathrm{IRake}}(\zeta)$ of an accurately measured multipath profile $s(t)$ given by

$$R_{\mathrm{IRake}}(\zeta) \approx \int_0^T s(t)s(t-\zeta)dt. \tag{12}$$

Examples of these correlation functions for the set of measurements from rooms P and H are shown in Fig. 11. As one would expect, when normalized to equal energy these correlation functions look approximately the same for values of the shift parameter $\zeta$ less than a pulse width ($< 1$ ns). However these correlation functions vary considerably for larger values of $\zeta$ because

the set of differential path delays varies for different points on the measurement grid. For large values of $\zeta$, these plots may look quite different for different rooms.

For the monocycle used to sound rooms and produce the curves of Fig. 11, a reasonable choice of the PPM data shift parameter $\delta$ is the location of the first aggregate minimum next to the peak in these curves, roughly 0.5 ns. Notice that the BER performance prediction will vary somewhat from position to position within the measurement grid because the correlation properties of the multipath profile will vary. This technique of using measured multipath profiles to evaluate signal designs has been used to compare different possible 4-ary PPM designs [10].

### *E. Selective Rake in a Multipath Environment*

The infinite Rake receiver is not realizable. In fact, as the resolution of a radio system becomes finer, performance approaching that of an infinite Rake receiver becomes more difficult to achieve. We can use propagation measurements made with a monocycle pulser to predict the performance of an impulse radio system, and that technique is described here for a single impulse radio link.

A selective Rake receiver is one that diversity combines the outputs of a fixed number of correlators, each correlator locked to the signal coming over a particular propagation path. The performance of a selective Rake impulse radio receiver with coherent diversity combining of $L$ correlator outputs, each correlator matched to an ideal reference template $w_{\rm rec}(t)$ for detecting binary PPM modulation, is shown in Fig. 12. For simplicity in this analysis, we have assumed that clocks and hop times are chosen so that no path is subject to interpulse interference. The technique used in constructing these curves was to determine from the multipath profile $s(t)$ how much received signal energy could be captured by a correlator as a function of its reference delay time, and to chose the reference delay times of the $L$ strongest measurements as the settings for selective Rake reception. The BER curves were then constructed using standard techniques.

The real payoff in selective Rake systems is the fact that system synchronization and communication can be maintained when a propagation path is broken, provided that other selected paths are not interrupted at the same time. Obviously the careful analysis of the likelihood of loss of system lock in a selective Rake system is a complex geometry-dependent problem.

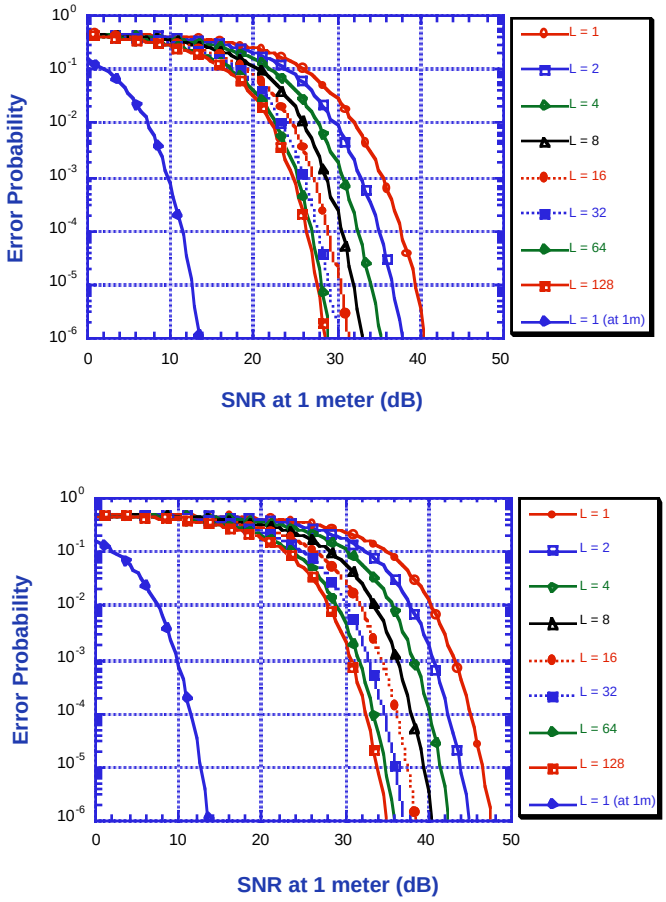


Fig. 12. Performance of Selective Rake receiver in rooms P (upper plot) and H (lower plot). These performance curves are averaged over the 49 measurements made in each room.

## IV. A Closing Comment

The potential of impulse radio to solve difficult indoor mobile communication problems is apparent because of its fine multipath resolution capability. As with most systems that push the capabilities of current technology, we believe that eventually (and quite possibly soon) impulse radio will become a practical solution to these problems.

## References

[1] R. A. Scholtz, "Multiple access with time-hopping impulse modulation," in *Proc. MILCOM*, Oct. 1993.

[2] J. M. Wozencraft and I. M. Jacobs, *Principles of Communication Engineering*. London: John Wiley & Sons, Inc., first ed., 1965.

[3] M. K. Simon, S. M. Hinedi, and W. C. Lindsey, *Digital Communication Techniques: Signal Design and Detection*. Englewood Cliffs, New Jersey 07632: Prentice Hall, first ed., 1995.

[4] H. V. Poor, "Signal processing for wideband communications," *IEEE Information Society Newsletter*, June 1992.

[5] S. Verdu, "Recent progress in multiuser detection," in *Multiple Access Communications: Foundations for Emerging Technologies*, pp. 164–175, IEEE Press, 1993.

[6] M. Z. Win, R. A. Scholtz, and L. W. Fullerton, "Time-hopping SSMA techniques for impulse radio with an analog modulated data subcarrier," in *Proc. IEEE Fourth Int. Symp. on Spread Spectrum Techniques & Applications*, Sept. 1996. Mainz, Germany.

[7] C. L. Weber, G. K. Huth, and B. H. Batson, "Performance considerations of code division multiple-access systems," *IEEE Trans. on Vehicul. Technol.*, vol. VT-30, pp. 3–9, Feb. 1981.

[8] M. Z. Win and R. A. Scholtz, "Ultra-wide bandwidth (UWB) time-hopping spread-spectrum impulse radio for wireless multiple access communications," *IEEE Trans. Commun.*, Jan. 1997. submitted.

[9] M. K. Simon, J. K. Omura, R. A. Scholtz, and B. K. Levitt, *Spread Spectrum Communications Handbook*. McGraw-Hill, Inc., revised ed., 1994.

[10] F. Ramirez-Mireles, M. Z. Win, and R. A. Scholtz, "Signal selection for the indoor wireless impulse radio channel," in *Proc. 47th Annual Int. Veh. Technol. Conf.*, May 1997.